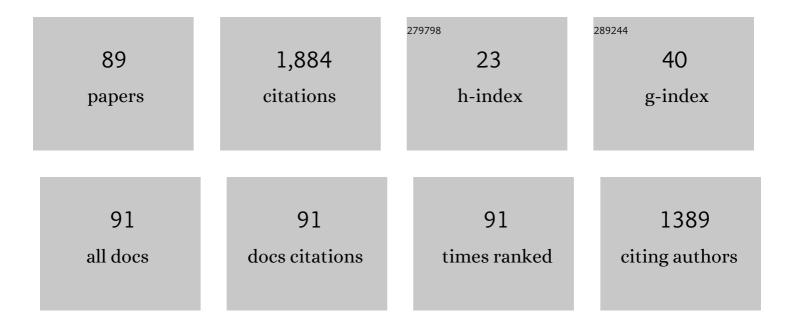
## Doug A Bennett

List of Publications by Year in descending order

Source: https://exaly.com/author-pdf/8622658/publications.pdf

Version: 2024-02-01



#	Article	IF	CITATIONS
1	Multiplexed Superconducting Detectors for a Neutrino Mass Experiment. IEEE Transactions on Applied Superconductivity, 2022, 32, 1-4.	1.7	0
2	Measurements of Strong-Interaction Effects in Kaonic-Helium Isotopes at Sub-eV Precision with X-Ray Microcalorimeters. Physical Review Letters, 2022, 128, 112503.	7.8	11
3	Absolute energies and emission line shapes of the L x-ray transitions of lanthanide metals. Metrologia, 2021, 58, 015016.	1.2	12
4	A microwave SQUID multiplexer optimized for bolometric applications. Applied Physics Letters, 2021, 118, .	3.3	21
5	A model for excess Johnson noise in superconducting transition-edge sensors. Applied Physics Letters, 2021, 118, .	3.3	8
6	Deexcitation Dynamics of Muonic Atoms Revealed by High-Precision Spectroscopy of Electronic <mml:math <br="" xmlns:mml="http://www.w3.org/1998/Math/MathML">display="inline"&gt;<mml:mi>K</mml:mi></mml:math> X Rays. Physical Review Letters, 2021, 127, 053001.	7.8	19
7	Design of a 3000-Pixel Transition-Edge Sensor X-Ray Spectrometer for Microcircuit Tomography. IEEE Transactions on Applied Superconductivity, 2021, 31, 1-5.	1.7	11
8	Progress in the Development of TES Microcalorimeter Detectors Suitable for Neutrino Mass Measurement. IEEE Transactions on Applied Superconductivity, 2021, 31, 1-5.	1.7	7
9	Transition-Edge Sensor Optimization for Hard X-ray Applications. IEEE Transactions on Applied Superconductivity, 2021, 31, 1-5.	1.7	6
10	Hyperspectral X-Ray Imaging: Progress Towards Chemical Analysis in the SEM. IEEE Transactions on Applied Superconductivity, 2021, 31, 1-6.	1.7	2
11	Dynamical Response of Transition-Edge Sensor Microcalorimeters to a Pulsed Charged-Particle Beam. IEEE Transactions on Applied Superconductivity, 2021, 31, 1-4.	1.7	2
12	Broadband high-energy resolution hard x-ray spectroscopy using transition edge sensors at SPring-8. Review of Scientific Instruments, 2021, 92, 013103.	1.3	14
13	Expanding the Capability of Microwave Multiplexed Readout for Fast Signals in Microcalorimeters. Journal of Low Temperature Physics, 2020, 199, 164-170.	1.4	0
14	Waveform Analysis of a 240-Pixel TES Array for X-Rays and Charged Particles Using a Function of Triggering Neighboring Pixels. Journal of Low Temperature Physics, 2020, 200, 269-276.	1.4	4
15	X-ray Spectroscopy of Muonic Atoms Isolated in Vacuum with Transition Edge Sensors. Journal of Low Temperature Physics, 2020, 200, 445-451.	1.4	13
16	Mitigating the Effects of Charged Particle Strikes on TES Arrays for Exotic Atom X-ray Experiments. Journal of Low Temperature Physics, 2020, 200, 247-254.	1.4	4
17	High Energy Background Event Identification Using Local Group Trigger in a 240-pixel X-ray TES Array. Journal of Low Temperature Physics, 2020, 200, 392-399.	1.4	2
18	Integration of a TES-based X-ray spectrometer in a kaonic atom experiment. Journal of Low Temperature Physics, 2020, 199, 1018-1026.	1.4	9

#	Article	IF	CITATIONS
19	Hyperspectral X-ray Imaging with TES Detectors for Nanoscale Chemical Speciation Mapping. Journal of Low Temperature Physics, 2020, 200, 437-444.	1.4	7
20	Development of a transition-edge sensor bilayer process providing new modalities for critical temperature control. Superconductor Science and Technology, 2020, 33, 115002.	3.5	10
21	Configurable error correction of code-division multiplexed TES detectors with a cryotron switch. Applied Physics Letters, 2019, 114, 232602.	3.3	3
22	High-Throughput, DC-Parametric Evaluation of Flux-Activated-Switch-Based TDM and CDM SQUID Multiplexers. IEEE Transactions on Applied Superconductivity, 2019, 29, 1-6.	1.7	8
23	Soft X-ray spectroscopy with transition-edge sensors at Stanford Synchrotron Radiation Lightsource beamline 10-1. Review of Scientific Instruments, 2019, 90, 113101.	1.3	40
24	A transition-edge sensor-based x-ray spectrometer for the study of highly charged ions at the National Institute of Standards and Technology electron beam ion trap. Review of Scientific Instruments, 2019, 90, 123107.	1.3	23
25	Crosstalk in microwave SQUID multiplexers. Applied Physics Letters, 2019, 115, .	3.3	15
26	Advances in Analysis of Microcalorimeter Gamma-Ray Spectra. IEEE Transactions on Nuclear Science, 2019, 66, 2355-2363.	2.0	4
27	Microwave SQUID multiplexing for the Lynx x-ray microcalorimeter. Journal of Astronomical Telescopes, Instruments, and Systems, 2019, 5, 1.	1.8	24
28	Development of space-flight compatible room-temperature electronics for the Lynx x-ray microcalorimeter. Journal of Astronomical Telescopes, Instruments, and Systems, 2019, 5, 1.	1.8	4
29	Lynx x-ray microcalorimeter. Journal of Astronomical Telescopes, Instruments, and Systems, 2019, 5, 1.	1.8	39
30	A 300-mK Test Bed for Rapid Characterization of Microwave SQUID Multiplexing Circuits. Journal of Low Temperature Physics, 2018, 193, 886-892.	1.4	0
31	Characterization of the microwave multiplexing readout and TESs for HOLMES. Journal of Physics: Conference Series, 2018, 1056, 012022.	0.4	Ο
32	A Scalable Readout for Microwave SQUID Multiplexing of Transition-Edge Sensors. Journal of Low Temperature Physics, 2018, 193, 485-497.	1.4	21
33	TES X-ray Spectrometer at SLAC LCLS-II. Journal of Low Temperature Physics, 2018, 193, 1287-1297.	1.4	21
34	A Highly Linear Calibration Metric for TES X-ray Microcalorimeters. Journal of Low Temperature Physics, 2018, 193, 249-257.	1.4	3
35	Microstructure Analysis of Bismuth Absorbers for Transition-Edge Sensor X-ray Microcalorimeters. Journal of Low Temperature Physics, 2018, 193, 225-230.	1.4	4
36	Toward Large Field-of-View High-Resolution X-ray Imaging Spectrometers: Microwave Multiplexed Readout of 28 TES Microcalorimeters. Journal of Low Temperature Physics, 2018, 193, 258-266.	1.4	16

#	Article	IF	CITATIONS
37	Highly-multiplexed microwave SQUID readout using the SLAC Microresonator Radio Frequency (SMuRF) electronics for future CMB and sub-millimeter surveys. , 2018, , .		28
38	A reassessment of absolute energies of the x-ray L lines of lanthanide metals. Metrologia, 2017, 54, 494-511.	1.2	35
39	A practical superconducting-microcalorimeter X-ray spectrometer for beamline and laboratory science. Review of Scientific Instruments, 2017, 88, 053108.	1.3	96
40	Dependence of transition width on current and critical current in transition-edge sensors. Applied Physics Letters, 2017, 110, .	3.3	20
41	Simultaneous readout of 128 X-ray and gamma-ray transition-edge microcalorimeters using microwave SQUID multiplexing. Applied Physics Letters, 2017, 111, .	3.3	75
42	Eliminating the non-Gaussian spectral response of X-ray absorbers for transition-edge sensors. Applied Physics Letters, 2017, 111, .	3.3	33
43	Beamline Test of a Transition-Edge-Sensor Spectrometer in Preparation for Kaonic-Atom Measurements. IEEE Transactions on Applied Superconductivity, 2017, 27, 1-5.	1.7	13
44	Microwave SQUID multiplexer demonstration for cosmic microwave background imagers. Applied Physics Letters, 2017, 111, .	3.3	40
45	Development of microwave-multiplexed superconductive detectors for the HOLMES experiment. Journal of Physics: Conference Series, 2016, 718, 062020.	0.4	2
46	Code-division-multiplexed readout of large arrays of TES microcalorimeters. Applied Physics Letters, 2016, 109, .	3.3	38
47	Absolute Energy Calibration of X-ray TESs with 0.04 eV Uncertainty at 6.4 keV in a Hadron-Beam Environment. Journal of Low Temperature Physics, 2016, 184, 930-937.	1.4	32
48	Developments in Time-Division Multiplexing of X-ray Transition-Edge Sensors. Journal of Low Temperature Physics, 2016, 184, 389-395.	1.4	103
49	Review of superconducting transition-edge sensors for x-ray and gamma-ray spectroscopy. Superconductor Science and Technology, 2015, 28, 084003.	3.5	230
50	Integration of TES Microcalorimeters With Microwave SQUID Multiplexed Readout. IEEE Transactions on Applied Superconductivity, 2015, 25, 1-5.	1.7	26
51	High-resolution X-ray emission spectroscopy with transition-edge sensors: present performance and future potential. Journal of Synchrotron Radiation, 2015, 22, 766-775.	2.4	59
52	Measurement of the240Pu/239Pu Mass Ratio Using a Transition-Edge-Sensor Microcalorimeter for Total Decay Energy Spectroscopy. Analytical Chemistry, 2015, 87, 3996-4000.	6.5	20
53	Phase-slip lines as a resistance mechanism in transition-edge sensors. Applied Physics Letters, 2014, 104,	3.3	18
54	High-Resolution Kaonic-Atom X-ray Spectroscopy with Transition-Edge-Sensor Microcalorimeters. Journal of Low Temperature Physics, 2014, 176, 1015-1021.	1.4	10

#	Article	IF	CITATIONS
55	Uncertainty of Plutonium Isotopic Measurements with Microcalorimeter and High-Purity Germanium Detectors. IEEE Transactions on Nuclear Science, 2014, 61, 2365-2372.	2.0	7
56	Integration of Radioactive Material with Microcalorimeter Detectors. Journal of Low Temperature Physics, 2014, 176, 1009-1014.	1.4	14
57	\$Q\$ Spectroscopy With Superconducting Sensor Microcalorimeters. IEEE Transactions on Nuclear Science, 2013, 60, 624-629.	2.0	14
58	Determination of Plutonium Isotopic Content by Microcalorimeter Gamma-Ray Spectroscopy. IEEE Transactions on Nuclear Science, 2013, 60, 681-688.	2.0	17
59	Observation of Bias-Specific Telegraph Noise in Large Transition-Edge Sensors. IEEE Transactions on Applied Superconductivity, 2013, 23, 2100203-2100203.	1.7	5
60	A Digital Signal Processing Module for Time-Division Multiplexed Microcalorimeter Arrays. IEEE Transactions on Applied Superconductivity, 2013, 23, 2500305-2500305.	1.7	3
61	Resistance in transition-edge sensors: A comparison of the resistively shunted junction and two-fluid models. Physical Review B, 2013, 87, .	3.2	20
62	Note: Operation of gamma-ray microcalorimeters at elevated count rates using filters with constraints. Review of Scientific Instruments, 2013, 84, 056107.	1.3	19
63	Microstrip filters for measurement and control of superconducting qubits. Review of Scientific Instruments, 2013, 84, 014706.	1.3	8
64	Identification and elimination of anomalous thermal decay in gamma-ray microcalorimeters. Applied Physics Letters, 2013, 103, 212602.	3.3	6
65	Table-Top Ultrafast X-Ray Microcalorimeter Spectrometry for Molecular Structure. Physical Review Letters, 2013, 110, 138302.	7.8	40
66	High-resolution gamma-ray spectroscopy with a microwave-multiplexed transition-edge sensor array. Applied Physics Letters, 2013, 103, 202602.	3.3	61
67	A high resolution gamma-ray spectrometer based on superconducting microcalorimeters. Review of Scientific Instruments, 2012, 83, 093113.	1.3	77
68	Current distribution and transition width in superconducting transition-edge sensors. Applied Physics Letters, 2012, 101, .	3.3	23
69	Ultra-high Resolution Alpha Particle Spectrometry with Transition-Edge Sensor Microcalorimeters. Journal of Low Temperature Physics, 2012, 167, 955-960.	1.4	8
70	A Two-Fluid Model for the Transition Shape in Transition-Edge Sensors. Journal of Low Temperature Physics, 2012, 167, 102-107.	1.4	33
71	Stability of Al-Mn Transition Edge Sensors for Frequency Domain Multiplexing. IEEE Transactions on Applied Superconductivity, 2011, 21, 203-206.	1.7	10
72	Superconducting Transition-Edge Sensor Microcalorimeters for Ultra-High Resolution Alpha-Particle Spectrometry. IEEE Transactions on Applied Superconductivity, 2011, 21, 207-210.	1.7	16

#	Article	IF	CITATIONS
73	Large microcalorimeter arrays for high-resolution X- and gamma-rayspectroscopy. Nuclear Instruments and Methods in Physics Research, Section A: Accelerators, Spectrometers, Detectors and Associated Equipment, 2011, 652, 302-305.	1.6	13
74	Optical efficiency of feedhorn-coupled TES polarimeters for next-generation CMB instruments. , 2010, ,		4
75	An analytical model for pulse shape and electrothermal stability in two-body transition-edge sensor microcalorimeters. Applied Physics Letters, 2010, 97, .	3.3	18
76	Improved Isotopic Analysis With a Large Array of Gamma-Ray Microcalorimeters. IEEE Transactions on Applied Superconductivity, 2009, 19, 536-539.	1.7	2
77	Microcalorimeter arrays for ultra-high energy resolution X- and gamma-ray detection. Journal of Radioanalytical and Nuclear Chemistry, 2009, 282, 227-232.	1.5	15
78	Decoherence in rf SQUID qubits. Quantum Information Processing, 2009, 8, 217-243.	2.2	24
79	A First Application of the FRAM Isotopic Analysis Code to High-Resolution Microcalorimetry Gamma-Ray Spectra. IEEE Transactions on Nuclear Science, 2009, 56, 2284-2289.	2.0	1
80	Large-Area Microcalorimeter Detectors for Ultra-High-Resolution X-Ray and Gamma-Ray Spectroscopy. IEEE Transactions on Nuclear Science, 2009, 56, 2299-2302.	2.0	33
81	Characterization of Thermal Cross-talk in a $\hat{1}^3$ -ray Microcalorimeter Array. , 2009, , .		Ο
82	Two-Body Models for Analyzing Complex Impedance. , 2009, , .		0
83	Cryogenic Microcalorimeter System for Ultra-High Resolution Alpha-Particle Spectrometry. , 2009, , .		2
84	Measurements of Bolometer Uniformity for Feedhorn Coupled TES Polarimeters. , 2009, , .		4
85	Issues in energy calibration, nonlinearity, and signal processing for gamma-ray microcalorimeter detectors. , 2009, , .		2
86	Substrate and process dependent losses in superconducting thin film resonators. Superconductor Science and Technology, 2008, 21, 075013.	3.5	41
87	rf-SQUID qubit readout using a fast flux pulse. Superconductor Science and Technology, 2007, 20, S445-S449.	3.5	20
88	Induced anisotropy and positive exchange bias: A temperature, angular, and cooling field study by ferromagnetic resonance. Physical Review B, 2002, 65, .	3.2	49
89	Magnetic anisotropy and interlayer coupling in Fe0.5Co0.5(100) films on GaAs(100). Journal of Applied Physics, 2001, 89, 7514-7516.	2.5	8